ABSTRACT

An accurate, reproducible, and affordable means to screen the increasing number of xenobiotics for toxic effects to the skin is imperative for accurate assessment of potential health risk. My goal was to investigate the effects of naphthalene in two three-dimensional (3D) human skin reconstruct models, a commercially available MatTek, EFT-400 model and our in-house grown JCB-110 model. These two reconstruct models were exposed to 1,250, 6,250, 12,500, or 31,250 nmol of naphthalene on exposure days 1, 3, and 5. Naphthalene and its metabolites were measured in tissue culture media using liquid chromatography–mass spectrometry with atmospheric pressure photoionization source. Naphthyl-keratin adducts were observed by immunohistochemistry using antibodies specific to 1-naphthyl and 2-napthyl modified keratin-1 and keratin-10 proteins. The results provide evidence that naphthalene was metabolized and sequestered within the epidermis and that penetration of naphthalene through the reconstructs was negligible. The JCB-110 reconstructs were cultured to contain melanocytes in addition to keratinocytes and fibroblasts while the EFT-400 only contained keratinocytes and fibroblasts. The addition of melanocytes in the JCB-110 model provide a more physiologically relevant model. The successful culturing of the reconstructs demonstrates the ability to produce a test system that is suitable for the screening of xenobiotics. This research will provide a means forward to evaluate and develop 3D human skin reconstruct models that are suitable for high-through put screening of dermally administered xenobiotics.

TABLE OF CONTENTS

LIST OF FIGURES

LIST OF TABLES

LIST OF ABBREVIATIONS

1,2-DHN	1,2-dihydroxynaphthalene
1,2-NQ	1,2-naphtholquinone
1,4-DHN	1,4-dihydroxynaphthalene
1,4-NQ	1,4-naphtholquinone
1,7-DHN	1,7-dihydroxynaphthalene
2,6-DHN	2,6-dihydroxynaphthalene
1-NAP	1-naphthol
2-NAP	2,naphthol
1NK1	1-naphthol-keratin-1
1NK10	1-naphthol-keratin-10
2NK1	2-naphthol-keratin-1
2NK10	2-naphthol-keratin-10
3D	3 dimensional
AD	atopic dermatitis
ADME	absorption, distribution, metabolism, and excretion
APCI	atmospheric-pressure chemical-ionization
APPI	atmospheric-pressure photoionization
DAPI	4',6-diamidino-2-phenylindole
DMEM	Dulbecco's modified eagle's medium
FITC	fluorescein isothiocyanate
FLG	filaggrin gene
FMO1	flavin-dependent monooxygenases 1
FMO2	flavin-dependent monooxygenases 2
HPLC	high-performance liquid chromatography
H&E	hematoxylin and eosin
IgG	immunoglobulin G
IHC	immunohistochemistry

IRB	institutional review board
K1	keratin-1
K10	keratin-10
LOQ	limit of quantification
LC-MS/MS	liquid chromatography – tandem mass spectrometry
MEM	minimum essential medium
MRM	multiple-reaction monitoring
NHDF	normal human dermal fibroblasts
NHEK	normal human epidermal keratinocytes
PAH	polycyclic aromatic hydrocarbons
PBPK	physiologically based pharmacokinetic
PBS	phosphate buffered saline
PTFE	polytetrafluoroethylene
PVDF	polyvinylidene fluoride
R^2	coefficient of determination
S/N	signal to noise ratio
SPE	solid phase extraction
UPLC	ultra-high-performance liquid chromatography
UVR	ultraviolet radiation

CHAPTER I

INTRODUCTION

1.1 Background

The current methods for investigating human dermal exposure to xenobiotics and the consequent toxicity and adverse effects are lacking a biologically relevant standard matrix for screening purposes. The recent report by National Academy of Sciences, Toxicity Testing in the 21st Century (NRC, 2007) has become the roadmap for the development and utilization of more predictive *in vitro* models of biological response in human risk assessment. The skin and the respiratory epithelium are the first sites of airborne environmental exposure and, thus, are both major targets for xenobiotic exposure and toxicity. The long-term objective of our laboratory is to increase the use of human tissues as surrogates for human exposures for evaluation of toxicity and safety assessment. Human tissue reconstruct assays can provide data for the identification of tissue-specific biomarkers and the development of computational toxicology, genomic, and bioinformatic analyses that aid in defining pathways of, and predict human toxicity to, the parent compounds and metabolites. Successful development of these tools will have the added benefit of decreasing the number and cost of animals required for preclinical toxicology and safety assessment. Furthermore, widespread use of human tissue reconstructs *in vitro* instead of monolayer cell cultures would be transformative, and would aid investigation of tissue-specific xenobiotic metabolism in exposed human populations. The human tissue reconstructs are also amenable to further development for high-throughput screening, genomic analysis of individual

susceptibilities, and computational toxicology, by maintaining cellular communication and physiology present in *in vivo* skin.

1.2 Skin: Structure and Function

My research focuses on the skin as a metabolic organ and route for systemic exposure and toxicity. The skin provides several very important functions including the regulation of the body's temperature and water balance, sensation, protection (physical barrier), and metabolism (Poet & McDougal, 2002). These multiple functional roles of the skin as well as its structural variations throughout the body and inter-individual differences make it a difficult experimental medium to obtain toxicity and metabolism data. This variation can be illustrated by comparing the thickness of the stratum corneum or the number of hair follicles per cm^2 in different areas of the body. The average stratum corneum thickness of the forearm is 16 μm, 400 μm for the palm, and 15 μm for the abdomen among men (Scheuplien & Blank, 1971). The average number of hair follicles at these sites is 95, 0, and 15 per cm^2, respectively (Snyder et al., 1992).

The skin consists of two distinct layers, the epidermis and the dermis. These two layers exhibit vastly different functions, and contain different cellular components. The relationship between these two layers is required for cellular communication, the exchange of nutrients, and absorption, detoxification, and/or excretion of xenobiotics. The outer most layer, the epidermis is a dynamic barrier that continually produces cornified cells and keratin to act as a physical barrier. Keratinocytes comprise >90% of the cells in the epidermal layer and are derived from the basal membrane of the epidermis, which differentiate into squamous cells, and eventually flake off (Eckert, 1991). This process of desquamation occurs continuously one cellular layer at a time in healthy skin. Keratinocytes produce a structural protein called keratin that serves as a

physical barrier and has the potential to sequester xenobiotics by adduction. In this manner, xenobiotics are eliminated from the body as the outer layers of the epidermis are shed. Another cell residing within the basal level of the epidermis is the melanocyte, which produces the pigment melanin for protection from ultraviolet radiation (UVR). The melanocyte secretes packets of melanin that are taken up by adjacent keratinocytes to protect their nuclei from UVR. In the proliferating basal layer, the melanocyte to keratinocyte ratio is 1:5. Melanocytes interact directly with keratinocytes through dendritic projections (Santiago-Walker et al., 2009). This process of delivering melanin through melanosome packets is an important process in the development of skin disease, and potentially in the absorption of xenobiotics. Therefore, keratinocytes and melanocytes are the first line of defense for dermal exposures.

The dermis consists primarily of fibroblasts and is much more structurally complicated than epidermis, containing pores and hair follicles that are derived in the dermis and efflux through the epidermis. Hair follicles and pores are potential routes for xenobiotics to gain entry into the dermis through the epidermis without interacting with the barrier properties of the epidermis. The dermis provides the structure and environment needed to support nerve and vascular networks and appendages required to support the epidermis (Eckert, 1991). Xenobiotics that penetrate through the epidermis into the dermis have a greater chance of being absorbed into systemic circulation and distributed throughout the body because of the network of blood vessels. The structural components of the dermis are supported by fibroblasts. The primary function of fibroblasts is the synthesis and remodeling of connective tissue proteins. In addition, fibroblasts secret collagenase and gelatinase, which function in remodeling of collagen fibrils (Eckert, 1991).

1.3 Models for Dermal Toxicity Testing

Dermal toxicity is generally assessed using animal, cell culture, and excised skin models. Each of these models provide important but limited information on dermal toxicity, and none are suitable for rapid screening for toxic effects of xenobiotics.

1.3.1 Animal Models

Animal models for investigating absorption, distribution, metabolism, and excretion (ADME) and the effects of xenobiotics in the skin are considered problematic. First, rodent skin is significantly different from human skin in its architecture and thus, may have considerably different response to xenobiotic exposure compared to human skin (Chilcott, 2008). The mouse epidermis is thin consisting of a monolayered basal compartment with about two to five layers of living suprabasal cells, compared to 5 to 10 layers of suprabasal cells in human skin (Schweizer, 1993). This difference alone changes the functionality of the skin by providing less of a barrier. The density of hair follicles in rodent skin is also different. Unlike in rodents, the hair follicles in human skin are distributed unevenly, thus, leaving areas of potential exposure with little or no follicles. Further, in mice the melanocytes are concentrated in the hair follicles in contrast to human skin, where melanocytes are present in the basal layer of the epidermis (Brohem et al., 2010).

1.3.2 *In Vitro* Cell-culture Models

Monolayer human cell-culture models exist in an undifferentiated state unlike the cells in human skin or three-dimensional (3D) skin reconstruct models and thus, cannot provide complete information regarding the skin's barrier function. The lack of differentiation provides an

exceptionally poor model with respect to the keratinocytes in the epidermis that exists in human skin in various states of differentiation. The presence of only one cell type also neglects intercellular communication and the processes that may led to disease from a systems biology stand point.

Monolayer cell cultures provide limited utility. However, they are inexpensive and can provide useful information on functions of a single cell type (Andreoli et al., 2003). For example, monolayer cell cultures may give insight into changes in protein expression under varying conditions. However, the homeostatic state of a monolayer cell culture is a drastically different environment than that of a dynamic environment consistent with human skin or 3D reconstructed skin models.

Transformed cell lines often used in monolayered cultures have an unlimited lifespan, allowing prolonged studies, but may not accurately represent the *in vivo* situation as the phenotype of transformed cells differs from that of normal cells (Foster et al., 2000). In addition, individual cell types may respond quite differently to a complex mixture like polycyclic aromatic hydrocarbons (PAH), as they may lack the requisite biotransformation enzymes (Andreoli et al., 2003). Similarly, cell lines may show altered expression of a range of secretory and signaling molecules (Forbes & Ehrhardt, 2005). Overall, there are inherent biases when using these kinds of experimental systems (Balharry et al., 2008).

1.3.3 *In Vitro* Skin Models

Because of the practical issues to investigate ADME processes using human subjects, excised pig skin and human cadaver skin have been used to test the toxicity and metabolism of xenobiotics and to provide input for physiologically based pharmacokinetic (PBPK) models. The physical

characteristics of pig skin make it the most suitable animal model for human skin toxicity studies. Similarities in the pig and human skin include a thick epidermis, similar hair follicle density, and lipid composition, while interfollicular muscle and apocrine rather than eccrine sweat glands are present in the pig skin. The areas of human skin most likely to be subject to toxic exposures such as the arms, legs, hands, face, and neck contain eccrine sweat glands. In addition, excised human skin and pig skin are both expensive and are not suitable for large-scale testing or for xenobiotic screening.

The use of excised human cadaver skin and human skin collected from cosmetic surgeries in research requires institutional review board (IRB) approval and patient consent. To obtain fresh samples at regular time intervals as well as to adhere to specific quality standards such as where on the body the sample was derived, age, gender, or race of the donor make it difficult to perform these types of studies (Hu et al., 2010).

Skin reconstructs are commonly used in medicine for covering wounds of patients (Regnier et al., 1998). Recently, the use of *in vitro* human skin constructs has been given a greater consideration in experimental toxicology studies and a number of commercially available 3D human skin reconstructs have become available for researchers. The 3D reconstructs are commonly comprised of two layers, the epidermis and the dermis. What makes reconstruct models 3D is the layering of the epidermis and dermis to create a full-thickness tissue of 0.5-1.0 mm to mimic the structure and functions of the human skin (Gibbs et al., 2007). To maintain the 3D form, the dermis consists minimally of fibroblasts imbedded in a collagen matrix topped by a layer of differentiating epidermal keratinocytes. Keratinocytes in this environment continue to differentiate. New cells proliferate in the basal layer and differentiate while moving towards the

surface, migrating away from sources of nutrients. These cells eventually form sacs of keratin and other proteins, void of a nucleus.

In our laboratory, we have developed standardized conditions for isolation of melanocytes, keratinocytes, and fibroblasts from neonatal foreskins and successfully produced full-thickness 3D human skin reconstructs using these three cell types. The human skin reconstructs made in our laboratory exhibit normal skin architecture consisting of a dermis of fibroblasts embedded in collagen and an epidermis of basal melanocytes and ≈10 layers of differentiated keratinocytes ending in a cornified layer. *In vitro* skin models have the major advantage that cells are cultured initially individually. This allows the manipulation of each cell type prior to including the cells into the complex reconstructs. The 3D reconstructs prepared in our laboratory also include melanocytes, which reside in the basal layer of the epidermis. In the future, the means to grow 3D reconstructs with other cellular components such as dendritic (e.g., Langerhans' cells) and endothelial cells, and sebaceous glands, may also be developed and used to acquire data on the effects of xenobiotic exposures. On the other hand, the biological life-span for skin reconstructs is limited to about four weeks. Potentially, this can be extended to three months if fibrin-based matrices are used (Del Rio et al., 2002). However, fibrin-based matrices are not as skin-like as collagen.

1.4. The Goal of the Study

My research focuses on skin as a metabolic organ and route for systemic exposure and toxicity. My objective for this study was to evaluate the 3D skin reconstructs grown in our laboratory as a model to screen for xenobiotic toxicity. Towards this objective, I aimed to demonstrate the metabolism of naphthalene as well as keratin adduction in the suprabasal layer of the skin reconstructs. Further evaluation of the skin grown in our laboratory was performed by comparing these results to commercially available 3D skin reconstructs. The information obtained from these experiments provides insight into how the 3D skin reconstructs currently perform as well as what modifications may be needed to improve the skin reconstructs and the techniques used for testing in order to provide a more physiologically relevant skin model.

CHAPTER II

MATERIALS & METHODS

2.1 Human 3D Full-thickness Skin Reconstructs

In order to explore the suitability of *in vitro* human 3D skin reconstructs for toxicity testing, I evaluated the penetration and effects of naphthalene exposure in two different reconstruct models; a commercially available full-thickness epidermis (EFT-400, MatTek, Ashford, MA, USA), which contains fibroblasts and keratinocytes, and our in-house grown full-thickness epidermis (JCB-110), which contains melanocytes in addition to fibroblasts and keratinocytes.

2.1.1 EFT-400 Skin Reconstructs

EFT-400 reconstructs are comprised of normal human epidermal keratinocytes (NHEK) derived from neonatal-foreskin tissue and normal human dermal fibroblasts (NHDF) derived from neonatal skin from a single donor. These cells are cultured *in vitro* to form a multilayered, highly differentiated model of full-thickness human epidermis. The reconstructs are grown in a proprietary medium containing Dulbecco's Modified Eagle's Medium (DMEM), growth factors, and hormones including epidermal growth factor, insulin, and hydrocortisone. Antibiotics (gentamicin), anti-fungal agent (amphotericin), as well as other additives such as lipid precursors are also included in the medium. The reconstructs are grown on a 1.2 cm diameter cellulose membrane (surface area 1.0 cm^2; pore size 0.4 μm) with the appropriate air-liquid interface in Costar Snapwell (Corning, Lowell, MA) 6-well tissue-culture plate inserts containing 1 mL of media.

2.1.2 JCB-110 Skin Reconstructs

JCB-110 reconstructs grown in our laboratory are comprised of NHEK, NHDF, and melanocytes isolated from neonatal foreskins. Each reconstruct is grown using the three cell types isolated from a single donor (i.e., they are isogenic). The addition of melanocytes to the reconstructs provides a tissue reconstruct that more closely resembles the *in vivo* human epidermis.

To prepare JCB-110 reconstruct, epidermis and dermis from the neonatal-foreskin are separated using an overnight dispase II digestion at 4°C. The epidermal sheath is minced and cells (i.e., keratinocytes and melanocytes) are dispersed using trypsin digestion. After deactivating trypsin, half of the epidermal cells are placed into either keratinocyte or melanocyte media for growth selection of each cell type. To obtain the fibroblasts, the dermis is minced and digested overnight at room temperature with collagenase. Fibroblasts are then grown in an appropriate growth medium.

The dermis for JCB-110 is created by preparing a thin acellular layer of collagen as a base for the cellular layer and to seal the insert so that the reconstruct can be grown under medium for a few days before airlift. This collagen matrix includes minimum essential medium (MEM, Life Technologies, Carlsbad, CA), L-glutamine (Life Technologies, Carlsbad, CA), fetal bovine (Sigma, St. Louis, MO) or supplemented calf serum (Thermo Scientific, San Jose, CA), sodium bicarbonate (Sigma, St. Louis, MO), and bovine collagen (Organogenesis, Canton, MA). After polymerization of the thin acellular collagen layer, a thicker cellular layer containing fibroblasts is added for the formation of dermis (volume 0.5 cm^3). During the formation of dermis, the fibroblasts interact with the collagen fibers and contract the collagen by up to 50X in

volume. The cellular dermis layer pulls away from the sides of the insert and creates a depression on its surface.

After 4 – 7 days of dermis growth, the epidermal cells are added to the surface of the dermis. Melanocytes and keratinocytes in a ratio of 1:5 are added to the surface of the dermis and are then grown under liquid medium for 4 days. After the cells are attached to the dermis and begin to form a basement membrane, the reconstructs are "airlifted" (i.e., liquid medium is removed from the surface of the reconstruct). Exposure to the air and change of media components (decrease concentration of epidermal growth factor (EGF) and increase of calcium) stimulate the keratinocytes to differentiate into a stratified layer. The skin reconstruct is mature in approximately 2 weeks after plating the epidermal cells and is stable for approximately a month in the tissue culture conditions.

2.2 Naphthalene Exposure

For evaluation of the human skin reconstruct models, I investigated the metabolism and keratin adduction of naphthalene in the skin reconstructs. Naphthalene, the simplest form of a polycyclic aromatic hydrocarbon (PAH), was chosen as a model compound because analytical methods for detection of naphthalene and its metabolites in urine are readily available (Waidyanatha et al., 2004; Egeghy et al., 2003; Serdar et al., 2003) . Naphthalene has also been shown to be a good quantitative biomarker of PAH exposure (Chao et al., 2005; Chao et al., 2006; Kim et al., 2007; Serdar et al., 2004; Serdar et al., 2003; Egeghy et al., 2003; Sobus et al., 2009a; Sobus et al., 2009b).

Naphthalene undergoes phase I metabolism by cytochrome P450 (P450) enzymes to an arene oxide (naphthalene-1,2-oxide) (Figure 1). Arene oxides are prime candidates for adduction

to proteins and DNA and are often used as biomarkers of exposure because of their affinity for free cysteins in hemoglobin and albumin. Arene oxides that are not adducted can be further metabolized by P450 isoenzymes to 1-naphthol (1-NAP), 2-naphthol (2-NAP), or 1,2-dihydro-1,2-dihydroxy naphthalene (1,2-DHN). These compounds can be eliminated or further metabolized to form glucoronides and other phase II metabolic products (Troester et al., 2002; Tingle et al., 1993; Wilson et al., 1996; Zheng et al., 1997)

Naphthalene-1,2-oxide in known to interact with keratin. Previously, we observed 1- and 2-naphthyl-keratin adducts in the tape-strip samples collected from the skin of fuel-cell maintenance workers who had been occupationally exposed to the jet fuel JP-8 (Kang-Sickel et al., 2008; Kang-Sickel et al., 2010; Kang-Sickel et al., 2011).

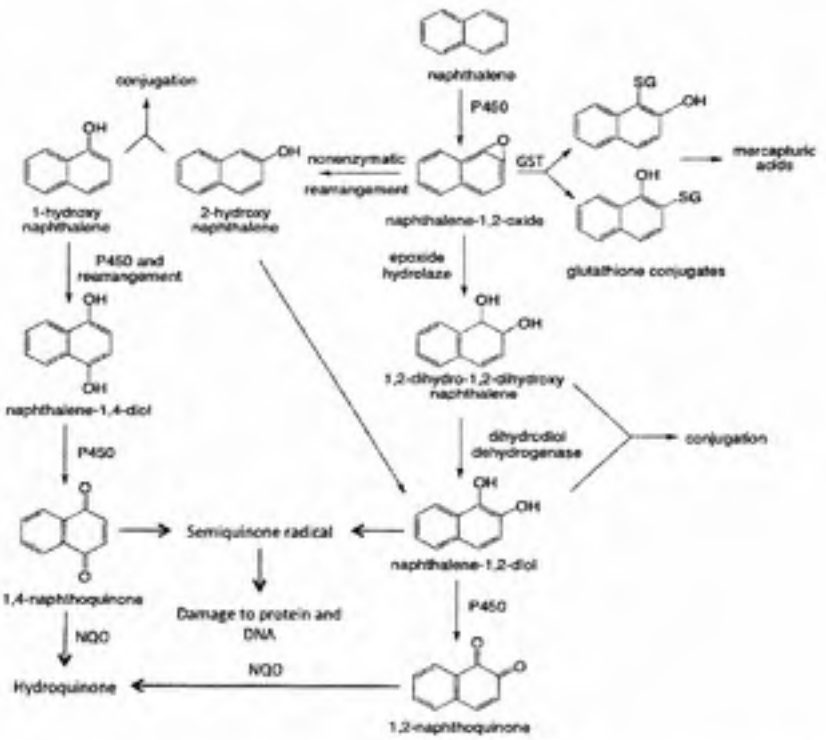

Figure 1. Proposed naphthalene metabolism in humans [adapted from Waidyanatha et al., 2004].

2.2.1 Preparation of Naphthalene Stock and Dosing Solutions

Naphthalene (Sigma, St. Louis, MO) was dissolved in acetone to achieve a concentration of 390 mg/mL. This stock solution was filter-sterilized by pressure-filtration system using a glass syringe and a polytetrafluoroethylene (PTFE) membrane in a stainless-steel filter holder (Swinny XX3001200, Millipore, Billerica, MA) and then stored at –80°C.

To prepare naphthalene dosing solution, the stock solution was allowed to thaw and warm to room temperature after which it was vortexed to dissolve any naphthalene that precipitated in the freezer. The stock solution was then serially diluted in acetone to achieve working solutions with concentrations of 15.6 µg/µL, 78 µg/µL, and 156 µg/µL.

2.2.2 Exposure and Sample Collection

Reconstructs were exposed three times every other day over the course of five days. One EFT-400 and one JCB-110 reconstruct received 10 µL of one of the naphthalene dosing solution at a concentration of 15.6 µg/µL, 78.0 µg/µL, 156 µg/µL, or 390 µg/µL, for an applied dose of 1250 nmol, 6,250 nmol, 12,500 nmol, and 31,250 nmol at each of the exposure days 1, 3, and 5. In addition, one EFT-400 and one JCB-110 reconstruct received acetone only exposure (negative control) while one EFT-400 and one JCB-110 were left untreated (unexposed control). Over the course of the 5-day exposure regime, one EFT-400 and one JCB-110 reconstruct received a total of 0.478 mg, 2.34 mg, 4.63 mg, or 11.7 mg naphthalene.

Tissue culture media (2 mL) was changed prior to the first naphthalene exposure in each tissue culture well and the used media was collected into an 8-mL glass vial and stored at –30°C for analysis (i.e., pre-exposure control). After 24-h of the first naphthalene exposure, the media (2 mL) was collected into an 8-mL glass vial and fresh media added into the well. The media

was changed daily and the used media was collected into an 8-mL glass vial and stored at –20˚C for analysis of naphthalene and its metabolites by liquid chromatography – tandem mass spectrometry (LC-MS/MS).

On day 6, the reconstructs were removed from the tissue culture wells and the reconstructs and the polycarbonate membranes were gently separated with forceps and stored in a glass vial until analysis. The dermis and epidermis were separated with forceps and placed in 2-mL glass vials and stored at –20˚C for further preparation and analysis by LC-MS/MS or the reconstructs were fixed in a 37% formaldehyde solution to be embedded in paraffin, and sectioned by the UNC Translational Pathology Laboratory for hematoxylin and eosin (H&E) staining and immunohistochemistry (IHC) analysis.

2.3 Analysis of Naphthalene and Its Metabolites

2.3.1 LC-MS/MS Method

LC-MS/MS analysis was performed using an ultra-performance LC (UPLC; Acquity, Waters, Milford, MA) separation system coupled with a TSQ quantum-ultra triple-quadrupole mass spectrometer (ThermoFinnigan, San Jose, CA) to analyze naphthalene and its metabolites in the tissue culture media. Naphthalene and the metabolite standards 1-NAP, 2-NAP, 1,2-DHN, 1,4-dihydroxynaphthalene (1,4-DHN), 2,6-dihydroxynaphthalene (2,6-DHN), 1,7-dihydroxynaphthalene (1,7-DHN), 1,2-naphtholquinone (1,2-NQ), and 1,4-naphtholquinone (1,4-NQ) were purchased from Sigma Aldrich (St. Louis, MO).

Chromatographic separation of naphthalene and its metabolites was achieved using a 2.1 x 150 mm Hypersil gold column packed with 3 µm particles (Thermo Scientific, San Jose, CA). Mobile phase A consisted of 0.1% formic acid in deionized water and mobile phase B contained

0.1% formic acid in methanol. The mobile phase was delivered from 0.0 to 2.0 min at a ratio of 45% mobile phase A and 55% mobile phase B, and then mobile phase B was increased linearly from 55% to 75% from 2.0 to 7.0 min, and from 75% to 95% from 7.0 to 7.5 min. This ratio was held for 1 min before returning to the initial conditions of 45% mobile phase A and 55% mobile phase B for 8.5 to 9.0 min.

The MS was first operated in positive atmospheric-pressure chemical-ionization (APCI) mode and multiple-reaction monitoring (MRM) data were collected for the parent to fragment ion transitions. Because only naphthalene metabolites were detected using APCI, this method was modified to use atmospheric-pressure photoionization (APPI) as the ionization source. This change allowed simultaneous detection of naphthalene and its metabolites using two segments. Segment 1 from 0.0 to 6.5 min and Segment 2 from 6.5 to 10 min were used for the parent to fragment ion transitions shown in Table 1.

Table 1. MS Parameters for Segment 1 and Segment 2 in APPI.

Segment 1	**Precursor m/z**	**Fragment 1 m/z**	**CE**	**Fragment 2 m/z**	**CE**	**Fragment 3 m/z**	**CE**
2-NAP, 1-NAP	145	91	30	117	17	127	21
1,2 –NQ, 1,4-NQ, 1,7-NQ, 2,6-NQ	159	77	35	103	34	131	16
1,2 –DHN, 1,4-DHN, 1,7-DHN 2,6-DHN	161	105	22	115	29	133	16
Segment 2							
Naphthalene	128	78	35	102	22	NA	NA
[^{13}C]Naphthalene	129	79	35	103	22	NA	NA

NA = not applicable
CE = collision energy

2.3.2 Purification and Concentration of Media Samples

In order to determine the most efficient technique to separate and concentrate naphthalene and its metabolites from the tissue culture media, four different methods were investigated using either ethyl acetate (Methods 1 – 2) or solid-phase extraction (Methods 3 – 4) as described below.

2.3.1.1 Ethyl Acetate Extraction

Preliminary experiments were conducted to determine the efficacy of ethyl acetate extraction of naphthalene and its metabolites from the media samples. It was observed that extraction with 100% ethyl acetate achieved a more complete separation between the aqueous and organic phase compared to a mixture of ethyl acetate and acetonitrile (2:1 v/v).

In Method 1, a spiked media sample was prepared, in triplicate, consisting of 2 mL of media and a 100 µL aliquot of 12.0 µg/mL 1-NAP, 15.6 µg/mL 2-NAP, and 20.0 µg/mL naphthalene in methanol to achieve final concentrations of 0.57 µg/mL, 0.74 µg/mL, and 0.95 µg/mL, respectively, in the sample. The samples were extracted 4 times with ethyl acetate (2 mL) and the extractions pooled (8 mL final volume). The ethyl acetate was then removed by nitrogen stream to dryness at room temperature and the sample reconstituted with 100 µL of methanol-water solution (50:50 v/v).

In Method 2, a spiked media sample was prepared, in triplicate, consisting of 2 mL of media and a 100 µL aliquot containing concentrations of 12.0 µg/mL 1-NAP, 14.4 µg/mL 2-NAP, 15.2 µg/mL 1,2-DHN, 11.6 µg/mL 2,6-DHN, and 20 µg/mL of naphthalene in methanol to achieve final concentrations of 0.57 µg/mL, 0.69 µg/mL, 0.72 µg/mL, 0.55 µg/mL, and 0.95 µg/mL, respectively, in the sample. Sodium acetate (1 mL of 0.1 M) was added to the samples and vortexed to adjust pH to 5 (the optimal range for the β-glucuronidase reaction) in the

samples. Each sample was extracted 4 times with 2 mL of ethyl acetate. The extracted ethyl acetate layers from the sample were pooled (8 mL final volume) and then evaporated to near dryness by nitrogen stream at room temperature. Methanol (300 µL) was then added to the vial, the sample vortexed, and transferred to an ultrafree-MC microcentrifuge tube with a polyvinylidene fluoride filter (PVDF 0.45 µm; Millipore, Billerica, MA) for centrifugation at 800 *g* for 1 min. Samples were transferred to high-performance liquid chromatography (HPLC) vials for analysis by LC-MS/MS.

2.3.1.2 Solid-phase Extraction

Solid-phase extraction (SPE) is commonly used to eliminate the salts and other polar chemicals that could potentially interfere with LC-MS/MS analysis of the samples. Because sample losses may occur during SPE extraction, I investigated the efficacy of this technique in spiked media samples.

This method (Method 3) was developed by first observing the elution profile of naphthalene, 1-NAP, 2, NAP, 1,2-DHN, and 2,6-DHN, using a 1 cc Oasis HLB SPE column (Waters Technology Corporation, Milford, MA). The column was prepared by running 1 mL of methanol followed by 1 mL of water through the column. A spiked media sample (1 mL) was then loaded onto the column before rinsing with 300 µL of water followed by ten volumes of methanol.

Method 3 was further improved using a 3 cc Oasis HLB SPE column (Waters Technology Corporation, Milford, MA) and implementing the information acquired from the previous experiment with the 1-cc column. The 3-cc column was prepared by running 2 mL of methanol followed by 2 mL of water through the column. Media samples were prepared in

triplicate, by spiking a 100-µL aliquot of 8.4 µg/mL 1-NAP, 10.0 µg/mL 2-NAP, 8.4 µg/mL 1,2-DHN, 13.24 µg/mL 2,6-DHN, and 20 µg/mL naphthalene into 2 mL of media to achieve final concentrations of 0.40 µg/mL, 0.48 µg/mL, 0.40 µg/mL, 0.62 µg/mL, and 0.95 µg/mL, respectively, in the sample. The 2 mL samples of spiked media were loaded onto a 3-cc Oasis HLB SPE column, the column was rinsed with 1 mL of water, followed by five rinses with 300 µL of 100% methanol. The fractions were collected directly into HPLC vials in order to determine the elution profiles of the spiked compounds.

Method 4, utilized [^{13}C]naphthalene (Sigma, Milwaukee, WI) as an internal standard and larger elution volumes to elute naphthalene and its metabolites in one fraction to aid in the quantitation of naphthalene and its metabolites. Before loading the spiked media samples, the columns were prepared as described in Method 3. The spiked media were then loaded in 2 mL aliquots onto three SPE columns. One additional column was prepared and loaded with untreated media to serve as a control. The spiked media samples and the blank media sample were eluted in four subsequent steps consisting of (1) 1 mL of water, (2) 300 µL of methanol, (3) 2 mL of methanol, and (4) 1 mL of methanol and each fraction was collected separately.

Standards were prepared with [^{13}C]naphthalene as follows. A stock internal standard solution of [^{13}C]naphthalene was made at the concentration of 1,000 µg/mL in methanol. A standard solution (Standard 1) was then prepared by diluting 1-NAP, 2-NAP, 1,2-DHN, naphthalene, and 40 µL of [^{13}C]naphthalene internal standard into 1,960 µL of methanol to achieve final concentrations of 8.4 µg/mL 1-NAP, 11.6 µg/mL 2-NAP, 8.4 µg/mL 1,2-DHN, 19.2 µg/mL naphthalene, and 20.0 µg/mL [^{13}C]naphthalene. A diluent solution (20.0 µg/mL [^{13}C]naphthalene) was also prepared by delivering 200 µL of [^{13}C]naphthalene internal standard into 9,800 µL of methanol to serially dilute standard 1 to prepare a 6-point standard curve.

Spiked media samples were prepared by adding 100 µL of the spiking solution (2.8 µg/mL 1-NAP, 3.9 µg/mL 2-NAP, 2.8 µg/mL 1,2-DHN, and 6.4 µg/mL naphthalene) followed by 40 µL of the [^{13}C]naphthalene internal standard solution (1,000 µg/mL) into 1,860 µL of media. A single blank media sample was prepared by adding 100 µl of methanol and 40 µL of the [^{13}C]naphthalene internal standard solution (1,000 µg/mL) into 1,860 µL of media. Final concentrations of 0.14 µg/mL 1-NAP, 0.20 µg/mL 2-NAP, 0.14 µg/mL 1,2-DHN, 0.32 µg/mL naphthalene, and 20 µg/mL [^{13}C]naphthalene in 2 mL of media were loaded onto the SPE column.

2.3.3 Determination of the Loss of Naphthalene and Its Metabolites during Sample Process

In order to determine the loss of naphthalene and its metabolites during the evaporation step in the sample processing, a spiking solution was prepared in methanol containing 1-NAP (8.4 µg/mL), 2-NAP (10.0 µg/mL), 1,2-DHN (8.4 µg/mL), 2,6-DHN (13.2 µg/mL), and naphthalene (20.0 µg/mL) and 100 µL volumes were spiked into a mixture of 2 mL of methanol and 2 mL of ethyl acetate, each in triplicate. The samples were then evaporated at room temperature under a nitrogen stream in 10-mL glass centrifuge tubes, reconstituted in 100 µL of methanol, and analyzed by LC-MS/MS. The concentrations of the reconstituted samples (100 µL) were then compared to the concentrations of compounds in the spiking solution.

As a potential alternative to evaporation under nitrogen stream, the loss of these compounds was evaluated during concentration by vacuum centrifugation (SC110A, Savant, Holbrook, NY). A spiking solution was prepared in methanol containing 8.8 µg/mL 1-NAP, 10.4 µg/mL 2-NAP, 9.2 µg/mL 1,2-DHN, 9.6 µg/mL 2,6-DHN, and 20.0 µg/mL naphthalene and 100 µL volumes were spiked into 1 mL of methanol and 1 mL of ethyl acetate, each in

triplicate. The samples were concentrated to near dryness by vacuum centrifugation in 2 mL glass vials and reconstituted in 100 µL of methanol. The concentrations of the reconstituted samples (100 µL) were compared directly to the concentration of the spiking solution to determine the loss of 1-NAP, 2-NAP, 1,2-DHN, 2,6-DHN and naphthalene during the concentration process.

2.3.4 Sample Preparation for LC-MS/MS Analysis

2.3.4.1 Media from EFT-400 and JCB-110

Media collected separately on each of the days 1 – 6 from the EFT-400 and JCB-110 reconstructs were analyzed individually using Method 4 SPE extraction and LC-MS/MS analysis. The harvested media prepared and analyzed from the EFT-400 reconstructs included exposures to 1,250 nmol, 6,250 nmol, 12,500 nmol, and 31,250 nmol of naphthalene. The harvested media prepared and analyzed from the JCB-110 reconstructs included only the 31,250 nmol naphthalene exposure. Samples were incubated with *β*-glucuronidase (191 units/mL; sulfatase activity 6 units/mL; *Helix pomatia*) for 4 h at 37°C before SPE extraction.

Media from both the EFT-400 and JCB-110 reconstructs were also pooled over the exposure period to include media collected from days 2 – 6. Pooled media from the EFT-400 and JCB-110 reconstructs at 31,250 nmol exposure as well as the media from the EFT-400 reconstructs at 6,250 nmol exposure were used for this experiment. Samples were incubated with *β*-glucuronidase (191 units/mL; sulfatase activity 6 units/mL; *Helix pomatia*) for 4 h at 37°C and concentrated by lyophilization from an initial pooled volume of approximately 10 mL to approximately 2 mL. The concentrated media samples were prepared by Method 4 SPE extraction and analyzed by LC-MS/MS.

2.3.4.2 Epidermis and Dermis of the EFT-400 Reconstructs

The separated dermis and epidermis samples were analyzed as follows. Two EFT-400 dermis samples dosed with 6,250 nmol of naphthalene three times over the course of 5 days were transferred to separate glass homogenization tubes (5 mL) and 1 mL of cell-lysis reagent (CelLytic M, Sigma-Aldrich) containing [^{13}C]naphthalene at a final concentration of 10 µg/mL was added into each tube. Samples were then homogenized by hand with a Teflon® pestle. After homogenization, a 100-µL aliquot of the sample was removed and filtered with an ultrafree-MC centrifugal filter for analysis by LC-MS/MS. The remainder of the sample was incubated at 37°C for 2 h with β-glucuronidase. After incubation, 100-µL aliquot of the sample was removed and filtered using ultrafree-MC centrifugal filter for analyzsis by LC-MS/MS. To the remaining sample, 1 mL of ethyl acetate was added, sample was vortexed, and then centrifuged for 5 min at 265 *g*. An aliquot of 100 µL was removed for analysis by LC-MS/MS. The remainder of the mixture was stored at room temperature for one week and then prepared for re-analysis by LC-MS/MS as described above.

Dermis samples (n = 2) from EFT-400 reconstructs dosed with 1,250 nmol of naphthalene three times over the course of 5 days were prepared for LC-MS/MS analysis. Each dermis was incubated in 500 µL of collagenase (1 mg/mL in phosphate buffered saline; Sigma, St. Louis, MO) overnight at 37°C after being spiked with [^{13}C]naphthalene internal standard (10 µg/mL). The dissolved tissues were then incubated in cell-lysis reagent overnight at room temperature. These samples were observed to be completely dissolved and, therefore, were not homogenized. Two aliquots of 100 µL were taken at the following timepoints: (1) before treatment with β-glucuronidase, (2) after treatment with β-glucuronidase, and (3) after extraction

with ethyl acetate. In addition, after one week (4) all the ethyl acetate was removed from the sample by transfer pipette and the remaining aqueous layer was (5) extracted with hexane. The collected samples at the timepoints (1) before treatment with β-glucuronidase, (2) after treatment with β-glucuronidase, (3) after extraction with ethyl acetate, (4) after one week in ethyl acetate, and (5) after one week in ethyl acetate and extraction with hexane were analyzed for naphthalene, 1-NAP, 2-NAP, 1,2-DHN, and 2,6-DHN by LC-MS/MS.

Two EFT-400 epidermis samples dosed with 1,250 nmol of naphthalene three times over the course of 5 days were treated with 500 µL of cell-lysis reagent, [^{13}C]naphthalene was added to achieve a final concentration of 10 µg/mL in the sample, and samples stored at 4°C for 1 week. To further digest the epidermis, 500 µL of trypsin was added to each sample and the samples incubated overnight at 37°C. The final [^{13}C]naphthalene internal standard concentration was 5 µg/mL. The samples (1 mL) were purified using Method 4 SPE extraction before analysis by LC-MS/MS. The JCB-110 dermis and epidermis samples were not analyzed in this study.

2.3.4.3 Skin Reconstruct Support Membrane

The two polycarbonate membranes supporting the EFT-400 reconstructs exposed to 6,250 nmol of naphthalene three times every other day were each placed into separate glass vials, extracted with 250 µL of methanol, and analyzed by LC-MS/MS.

2.4 Immunohistochemistry

Immunohistochemistry (IHC) was performed to investigate naphthyl-keratin adduct formation in the epidermis of EFT-400 and JCB-110 reconstructs. To accomplish this, tissues treated with naphthalene at 1,250 nmol, 6,250 nmol, 12,500 nmol, or 31,250 nmol three times every other day

as well as the tissue treated with acetone vehicle and the negative control tissue were fixed with a solution containing six parts of 100% ethanol, three parts of water, and one part formalin (37% formaldehyde solution) before being dehydrated, embedded in paraffin, and sectioned by the UNC Translational Pathology Laboratory.

2.4.1 Deparaffinization and Rehydration

Deparaffinization was accomplished by subsequently submerging the slides in xylene twice (5 min each), 100% ethanol (3 min), 95% ethanol (3 min), 70% ethanol (3 min), 50% ethanol (3 min), and twice in 1X DAKO autobuffer solution (Carpinteria, CA) for 5 min. This process was followed by steaming the slides with decloaking agent (Biocare Medical, Concord, CA) for 30 min. Slides were placed on the bench top to cool for 10 min and rinsed with running water (Nanopure, Barnstead, Dubuque, IA) for 10 min. The slides were then submerged in 1X DAKO autobuffer for 5 min.

2.4.2 Blocking

A solution of 1% BSA was prepared in 1X DAKO autobuffer to be used as a blocking solution. The slides were placed in a blocking/staining chamber lined with wet paper towels to protect the slides from ambient light and to retain moisture. The blocking/staining chamber consisted of a plastic container with ridges to place each slide face up and a lid. After placing the slides into the chamber, each section (two per slide) was covered with approximately 50 µL of the 1% BSA blocking solution. The slides were removed after 45 min and briefly rinsed in 1X DAKO autobuffer by submerging in the solution and agitating slightly.

2.4.3 Staining

Antibodies specific to 1-naphthyl and 2-naphthyl-modified keratin-1 (K1) and keratin-10 (K10) proteins (Kang-Sickel et al., 2008) at the concentration of 955 μg/mL for 1-naphthyl-K1 (1NK1), 539 μg/mL for 2-naphthyl-K1 (2NK1), 644 μg/mL for 1-naphthyl-K10 (1NK10), and 709 μg/mL for 2-naphthyl-K10 (2NK10) were each diluted to a concentration of 50 μg/mL with 1% BSA. The 1NK1, 1NK10, 2NK1, and 2NK10 antibodies (100 μL; 50 μg/mL) were applied to each tissue section, the slides were carefully dried with a Kimwipe (Kimberly-Clark®) to avoid further dilution of the antibody after introduction to the slides, after which the slides were incubated for 1 h at room temperature. Each slide was then rinsed with DAKO autobuffer by transfer pipette prior to submerging in DAKO autobuffer to avoid contamination of the rinse solution. The secondary antibody, goat anti-rabbit immunoglobulin G (IgG; Alexa Flour 488; Invitrogen, Eugene,OR) was diluted to a concentration of 40 μg/mL from the stock (2 mg/mL) with 980 mL of 1% BSA and 20 μL of stock. The secondary antibody was applied to each slide section at a volume of 100 μL and incubated in the blocking/staining chamber for 1 h at room temperature. Each slide was then submerged in phosphate buffered saline (PBS; Mediatech Inc., Manasses, VA), three times for 5 min, the slides were dipped in and out of the PBS to agitate. The edges of each slide were dried with a Kimwipe and slides placed in the dark (blocking/staining chamber).

2.4.4 Coverslipping and Photography

The sections of a tissue were coverslipped by applying one drop (approximately 25 μL) of Vectashield hard-mounting medium with 4',6-diamidino-2-phenylindole (DAPI) (Vector Laboratories, Burlingame, CA) to the section. The coverslip was then carefully placed over the

section and placed back in the blocking/staining chamber. After the mounting medium began to set, the edges of the coverslips were coated with nail polish to occlude from air.

The slides were observed after the staining process under the inverse microscope (Olympus IX70) fitted with a Sony DXC-s 500 camera. The naphthol adducts that were tagged with the Alexa Flour 488 secondary antibodies were filtered using the fluorescein isothiocyanate (FITC) fluorescent filter and the cell nuclei stained with DAPI were observed with the DAPI filter. The two images were then overlayed to create a composite of the two images.

CHAPTER III

RESULTS

3.1 Analysis of Naphthalene and Its Metabolites

3.1.1 LC-MS/MS Method

The LC-MS/MS method developed provides good sensitivity and linearity among naphthalene and its metabolites 1-NAP, 2-NAP, 1,2-DHN/1,2-NQ, and 2,6-DHN/2,6-NQ. The limit of quantification (LOQ), signal to noise ratio (S/N), coefficient of determination (R^2), and retention times for these compounds are presented in Table 2. The R^2 value is given with and without the use of [^{13}C]naphthalene as an internal standard. Both 1-NAP and 2-NAP, as well as 1,2-DHN/1,2-NQ, and 2,6-DHN/2,6-NQ share the same molecular weights and fragmentation patterns and could not be identified by mass alone. However, this method provides a good chromatographic resolution between the metabolites making identification possible (Figure 2), except in the case of the hydroxyl naphthalenes and quinones. It was observed that the hydroxyl naphthalenes are oxidized to quinones and therefore are indistinguishable. For example 1,2-DHN shares the same fragmentation pattern as 1,2-NQ.

Table 2. Standards Analyzed by LC-MS/MS with APPI.

	Naphthalene	**1-NAP**	**2-NAP**	**1,2-DHN/ 1,2-NQ**	**2,6-DHN/ 2,6-NQ**
Limit of Quantification (µg/mL)	0.082	0.006	0.007	0.007	0.005
Signal to Noise Ratio (S/N)	96	84	86	15	108
R^2 without Internal Standard	0.9909	0.9870	0.9917	0.9920	0.9917
R^2 with Internal Standard	0.9977	0.9992	0.9996	0.9992	NA
Retention Time (min)	8.07	5.32	4.92	2.17	2.52

NA = not analyzed

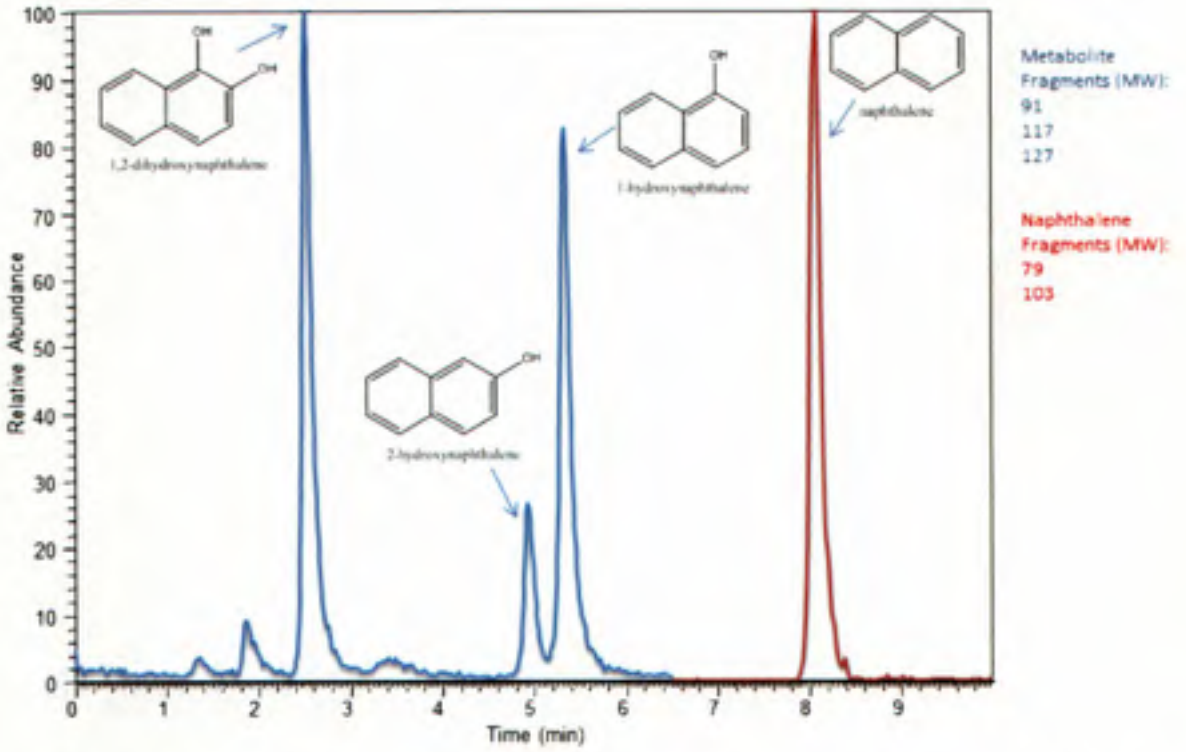

Figure 2. The chromatogram of naphthalene and its three metabolites in spiked media after Method 4 SPE extraction.

3.1.2 Purification and Concentration of Media Samples

3.1.2.1 Ethyl Acetate Extraction

Methods 1 and 2 did not prove successful due to poor recovery of naphthalene and its metabolites from the media (Table 3). Method 2, a modification of Method 1 by elimination of excessive glassware and solution transfers, had less variability than Method 1 but yielded no overall improvement in recovery. The poor recovery in both methods indicated that ethyl acetate is not a suitable solvent for extraction of naphthalene and its metabolites. This may be due to the large volume needed for the extraction, which translates to longer concentration time and potential losses of compounds due to evaporation.

A significant loss of the compounds during the sample concentration process was observed, which included evaporation under nitrogen stream at room temperature and centrifugation in the speed vacuum (Table 4). Since considerable differences in recovery were observed between the compounds, the poor recoveries are more likely due to the innate properties of the individual compounds than systematic losses of the whole samples during sample processing. For example, these compounds can have differences in volatility and/or partitioning into ethyl acetate. To demonstrate the loss of analyte during the concentration process, the analytes were spiked directly into methanol and ethyl acetate and the samples were concentrated under nitrogen stream, as well as by speed vacuum in both methanol and ethyl acetate. These recoveries were consistent with the recoveries observed in Method 2 (Table 3).

Table 3. Recovery (%) of naphthalene and its metabolites from spiked media using the different extraction methods.

Method	Naphthalene	1-NAP	2-NAP	1,2-DHN/ 1,2-NQ	2,6-DHN/ 2,6-NQ
Ethyl Acetate (Method 1)	12.6 ± 16.5	56.1 ± 14.1	12.6 ± 13.7	NA	NA
Ethyl Acetate (Method 2)	25.4 ± 26.2	40.6 ± 3.7	41.4 ± 3.6	56.5 ± 34.2	22.1 ± 17.1
SPE (Method 3)	64.0	30.9	36.5	114.8	100.9
SPE (Method 4)	77.3 ± 1.4	81.8 ± 0.6	89.0 ± 1.4	83.1 ± 5.6	NA

SPE solid phase extraction

NA = not analyzed

Table 4. Recovery (%) of naphthalene and its metabolites during sample concentration.

Method	Naphthalene	1-NAP	2-NAP	1,2-DHN/ 1,2-NQ	2,6-DHN/ 2,6-NQ
Methanol (RT)	35.9 ± 4.6	28.6 ± 1.7	32.4 ± 3.7	51.8 ± 4.4	53.9 ± 3.0
Methanol (SV)	58.7 ± 8.7	17.6 ± 2.0	18.3 ± 1.8	43.6 ± 3.0	91.0 ± 10.3
Ethyl Acetate (SV)	20.2 ± 10.6	5.7 ± 9.2	15.2 ± 3.2	36.6 ± 13.2	93.1 ± 10.6

RT room temperature; SV speed vacuum

3.1.2.2 Solid Phase Extraction

As an alternative to extraction by ethyl acetate and concentration with methanol and ethyl acetate, SPE was used to eliminate the salts and polar chemicals in the media before analysis by LC-MS/MS. Methods 3 and 4 provided better recovery for naphthalene and its metabolites than the solvent extraction in Methods 1 and 2 (Table 3). Method 3 was aimed to elute naphthalene and its metabolites in one small volume to obtain a sufficiently high concentration for greater sensitivity in LC-MS/MS analysis. This distribution is shown in Table 5.

Table 5. Recovery (µg) of naphthalene and its metabolites by fraction using SPE Method 3.

Fraction	Naphthalene[1]	1-NAP	2-NAP	1,2-DHN/1,2-NQ	2,6-DHN/2,6-NQ
1	1.419[1]	0.000	0.000	0.000	0.063
2	0.513[1]	0.000	0.036	2.186	8.277
3	1.913	0.892	1.381	3.426	4.502
4	4.949	1.071	1.449	2.195	0.972
5	3.080	0.531	0.662	0.723	0.130
6	1.374	0.163	0.187	0.134	0.003
Average	13.248	2.657	3.715	8.664	13.946
Percent Recovered	64.0	30.9	36.5	114.8	100.9

[1] Naphthalene measured in fractions 1 and 2 may be due to residual left from the previous clean-up procedure.

These elution profiles provide insight into the concentration of the fractions collected and how the volumes could be altered to maximize the concentration of naphthalene and the metabolites 1-NAP, 2-NAP, 1,2-DHN, and 2,6-DHN. The sum of the fractions in Table 5 was used to calculate the overall recovery using Method 3 (Table 3).

The using of the internal standard [^{13}C]naphthalene provided increased linearity and a means to normalize sample losses during the extraction process. Naphthalene eluted from the SPE column identically to [^{13}C]naphthalene internal standard (Table 6). However, the slightly different elution profiles of naphthalene from its metabolites did not provide an accurate means

to quantify the naphthalene metabolites when separated by SPE (data not shown). Analysis of 1-NAP, 2-NAP, and 1,2-DHN recovery was not feasible because of their partial elution during the methanol wash. This caused significant bias in the ratio of the [^{13}C]naphthalene internal standard and the metabolite level.

Table 6. Recovery of naphthalene from spiked tissue culture media (2 mL) using [^{13}C]naphthalene as an internal standard.

Sample Spike	Recovered (µg)	Percent Recovered
1	1.99	99.3
2	2.01	100.4
3	2.04	102.2
Average	**2.01**	**100.63**
Standard Deviation	**0.03**	**1.45**

3.1.3 LC-MS/MS Analysis of the Samples

3.1.3.1 EFT-400 and JCB-110 Media

Naphthalene was observed to be present in the tissue culture media collected from the wells of exposed ETF-400 reconstructs (Table 7 and Figure 3). The amount of naphthalene that reached the media increased overtime with respect to the exposure concentration and the number of days after naphthalene was applied (Table 7). The percentage of naphthalene recovered in the media is shown in Table 9. The data presented is calculated to show the total amount of naphthalene present in each media sample (µg). The sum of naphthalene collected over the 5-day exposure period for the 1,250, 6,250, 12,500, and 31,250 nmol exposures was 1.10 µg, 2.02 µg, 5.19 µg, and 9.69 µg, respectively.

Table 7. The amount of naphthalene (µg) in EFT-400 media collected after each naphthalene exposure.

Day/Naphthalene Dose	1,250 nmol	6,250 nmol	12,500 nmol	31,250 nmol
Day 1	0.094	0.132	0.511	1.217
Day 2	0.078	0.079	0.562	0.984
Day 3	0.317	0.707	1.167	2.382
Day 4	0.307	0.516	1.096	2.042
Day 5	0.302	0.586	1.850	3.068
Total	1.098	2.02	5.186	9.693

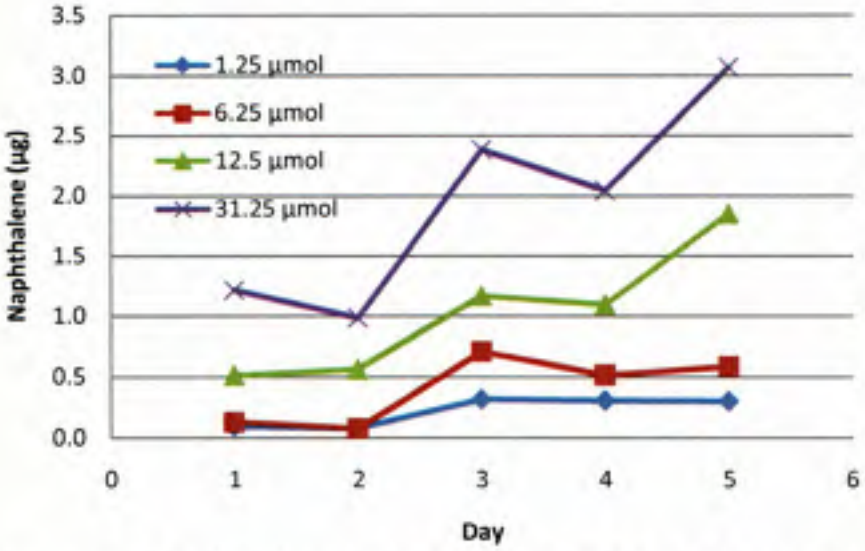

Figure 3. The amount of naphthalene (µg) measured in EFT-400 media during the 5-day exposure period (n = 1 for each point).

Naphthalene was observed to be present in the tissue culture media collected from JCB-110 reconstructs as shown in Table 8 and Figure 4. The data presented is calculated to show the total amount of naphthalene (µg) present in each sample. Similar to the EFT-400, the concentrations of naphthalene in JCB-110 trend positively over time with respect to all exposure concentrations. The amount of naphthalene measured in the media collected daily was similar between EFT-400 and JCB-110 reconstructs (Table 8).

Table 8. Total amount of naphthalene recovered (µg) in EFT-400 and JCB-110 media after exposure to 31,250 nmol of naphthalene three times every other day.

Day	EFT-400	JCB-110
Day 1	1.217	1.275
Day 2	0.984	1.017
Day 3	2.382	2.208
Day 4	2.042	2.031
Day 5	3.068	2.985
Total	9.693	9.516

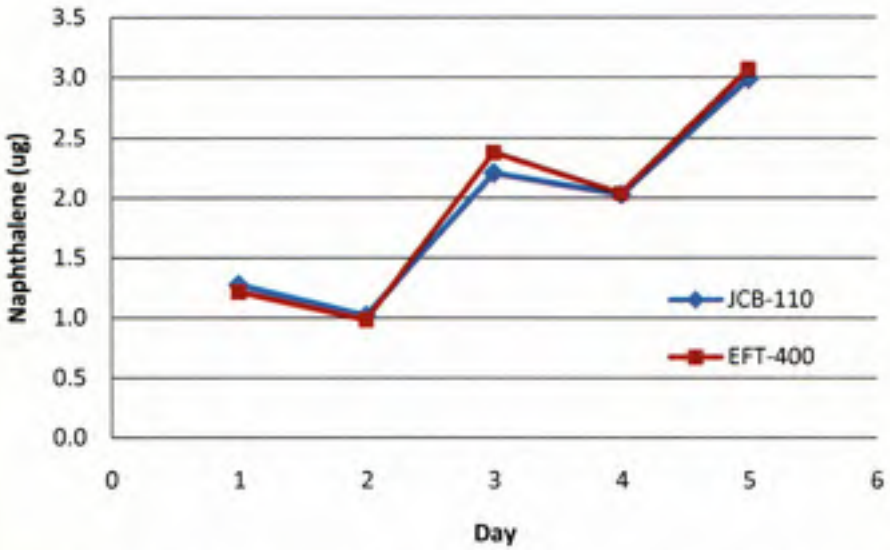

Figure 4. The total amount of naphthalene (µg) measured in EFT-400 and JCB-110 reconstructs during the 5-day exposure period (n = 1 for each point).

The pooled EFT-400 media samples also indicated a presence of 1,2-DHN (data not shown). The peak at 2.67 min is consistent with the retention time and the LC-MS/MS fragmentation pattern seen in the 1,2-DHN standard (Figure 5). The peak at 2.67 min is not present in the blank media sample (Figure 4). A very small amount of 1,2-DHN/1,2-NQ was observed in the media from the individually sampled media. However, it was difficult to determine if the presence of 1,2-DHN was indeed 1,2-DHN or just some other material

associated with the media itself. The pooled material indicated that there was 1,2-DHN in the media that was associated with the naphthalene dose. The amount of 1,2-DHN in the pooled 31,250 nmol dose media sample was estimated to be 0.56 µg and 0.6% of the applied dose.

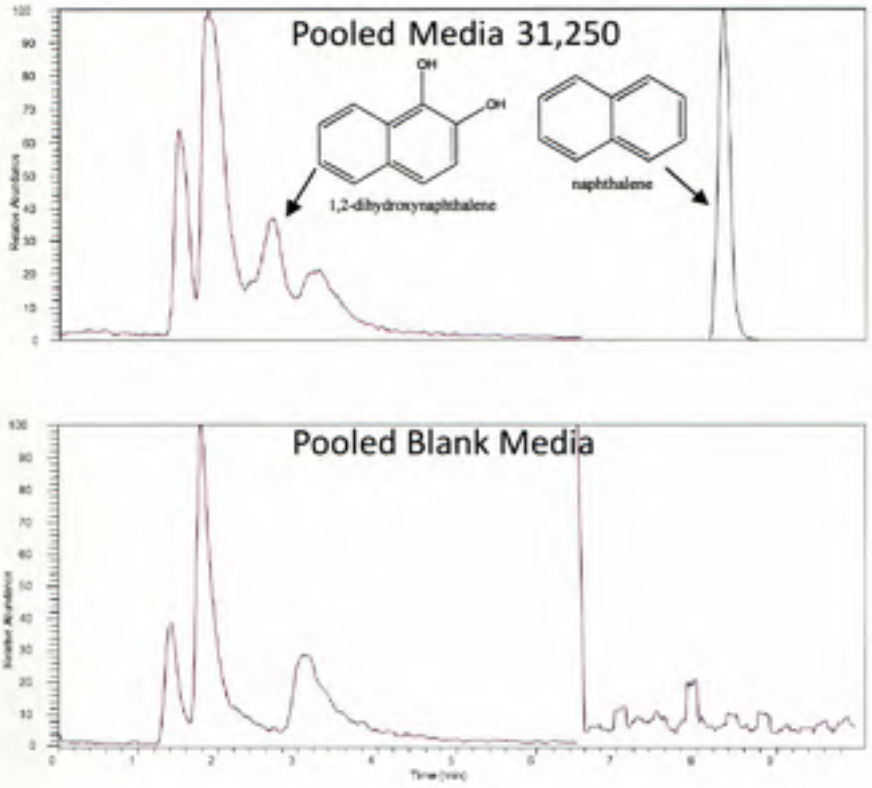

Figure 5. Spectra (Fragments MW 105, 115, 133) of a pooled media sample collected from the EFT-400 reconstruct exposed to 31,250 nmol of naphthalene.

Each of the three replicate samples of the pooled media from the JBC-100 reconstructs had an average recovered naphthalene amount of 3.99 µg and 0.06 µg of 1,2-DHN. No other metabolites were measured in these pooled media samples. This analysis was also performed using one EFT-400 reconstruct exposed to 31,250 nmol of naphthalene that showed a recovery of 6.75 µg of naphthalene and 0.56 µg of 1,2-DHN.

3.1.3.2 EFT-400 and JCB-110 Reconstructs

No naphthalene or its metabolites were observed in the dermis or epidermis of the exposed EFT-400 reconstructs. Further, the [^{13}C]naphthalene internal standard could not be recovered consistently from these reconstructs. The best recovery of the [^{13}C]naphthalene internal standard was after the dermis had been dissolved into a solution of collagenase, cell-lysis reagent, and then exposed to ethyl acetate for one week. Naphthalene and its metabolites could potentially be associated with the cell membrane, collagen, or other lipophilic regions of the dermis and epidermis and, thus, unavailable for extraction from the tissues.

3.1.3.3 Skin Reconstruct Support Membrane

An average of 3.28 µg of naphthalene was recovered from the polycarbonate membranes that supported the EFT-400 reconstructs. That amount of naphthalene was more than what was measured in the media at the 6,250 nmol dose level.

3.1.3.4 Summary of Naphthalene Disposition

Naphthalene was observed to be present only in small amounts in the media and the support membrane. These results are summarized in Table 9 as the percent of applied naphthalene that was detected by LC-MS/MS.

Table 9. The percent of naphthalene in the media collected over the 5 days of exposure to naphthalene from the EFT-400 or JCB-110 wells.

Total Applied Naphthalene over 5 Days (nmol)	JCB-110 Media [1]	EFT-400 Media [1]	JCB-110 Media Pooled Over 5 Days and Lyophilized	EFT-400 Media Pooled Over 5 Days and Lyophilized	EFT-400 Membrane
3,750	NA	0.23	NA	NA	NA
18,750	NA	0.08	NA	NA	0.14
37,500	NA	0.11	NA	NA	NA
93,750	0.08	0.08	0.03	0.06	NA

NA = not analyzed
[1]The media samples were collected and analyzed individually in days 1 – 6.

3.2 Immunohistochemistry

Observations of EFT-400 reconstructs illustrates a dose response in relation to all four naphthyl-keratin adducts (1NK1, 1NK10, 2NK1, and 2NK10). This response is shown below for the 2NK1 and 2NK10 treated reconstructs (Figures 6 and 7). The results indicate that metabolism takes place within the skin reconstructs and that the metabolites 1-NAP and 2-NAP did not efflux through the skin and into the media. Instead, these metabolites were adducted to keratin proteins.

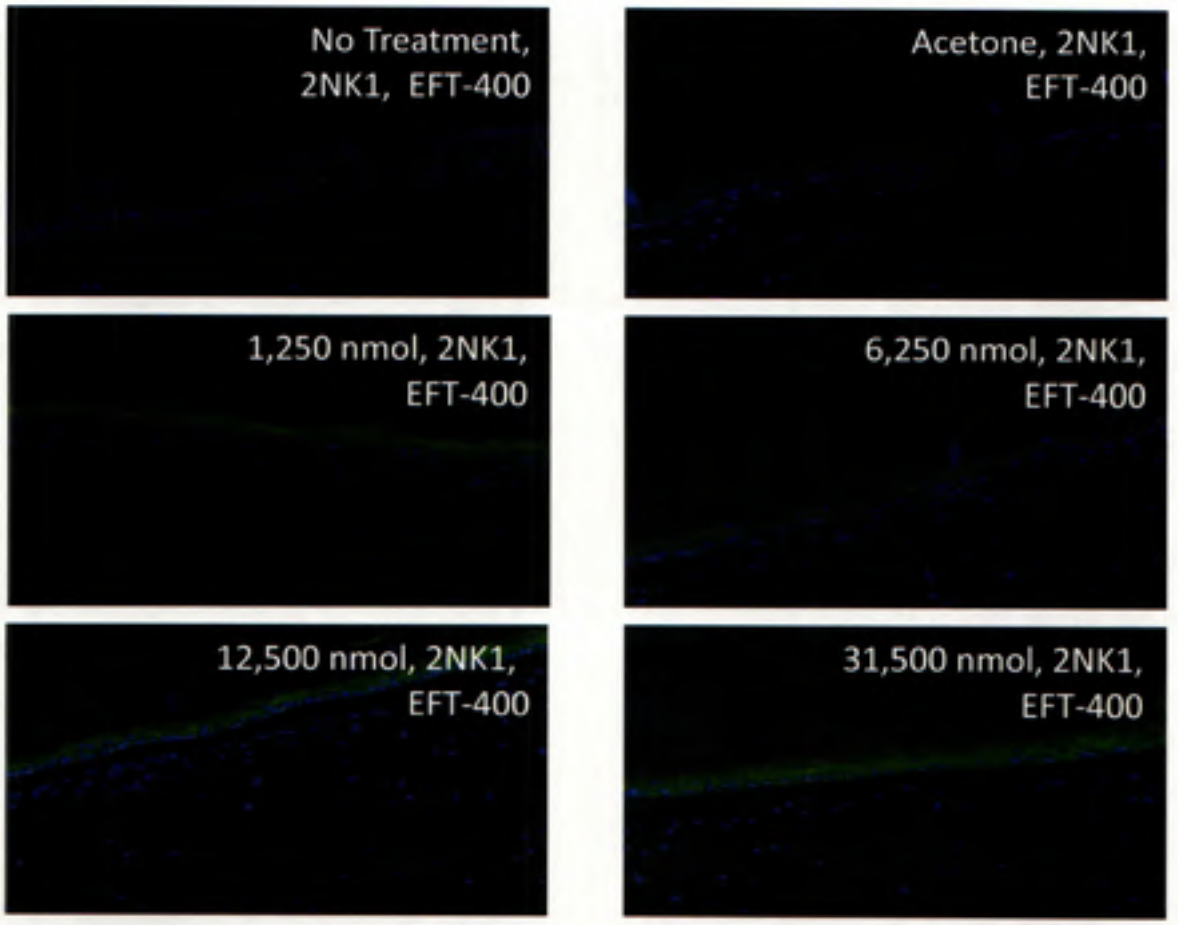

Figure 6. A dose-related increase in detectable 2NK1 adduct levels was observed in the epidermis, but not in the dermis of MatTek EFT-400 skin reconstructs, after three topical exposures to naphthalene (every other day). Anti-2NK1-green (Alexa Fluor 488); nuclear DNA-blue (DAP-1).

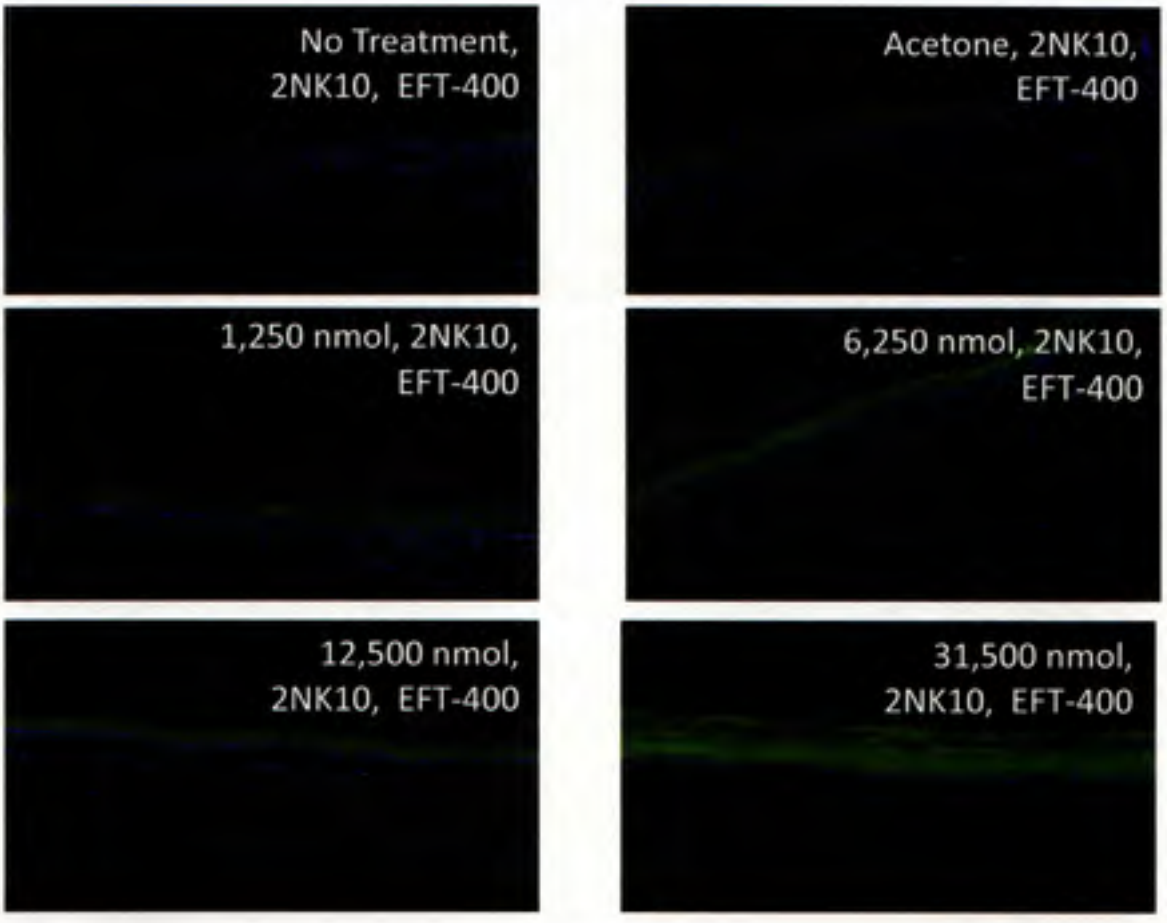

Figure 7. A dose-related increase in detectable 2NK10 adduct levels was observed in the epidermis, but not in the dermis of EFT-400 skin reconstructs, after three topical exposures to naphthalene (every other day). Anti-2NK10-green (Alexa Fluor 488); nuclear DNA-blue (DAP-1).

The JCB-110 and EFT-400 reconstructs were stained simultaneously and photographs were taken on the same day to limit fluorescence intensity variation between experiments caused by fluorescence quenching over time. Three dose levels were observed in this way and are presented in Figures 8 (no treatment), 9 (1,250 nmol), and 10 (31,250 nmol). Antibodies for 1N1K and 2N1K were used in this examination. A dose-response can be clearly seen with in the EFT-400 reconstructs (Figures 6 and 7). The number of cells observed in the dermis (fibroblasts) of the JCB-110 compared to the EFT-400 are more concentrated while the thickness

of the dermis is thinner in the JCB-110. The stratum corneum of the JCB-110 appears to be less uniform than the stratum corneum of the EFT-400 reconstructs. The uniformity of the JCB-110 stratum corneum is less apparent in the no treatment photographs (Figure 8), and begins to become thinner and more variable in the 31,250 nmol exposure level (Figure 10). The distinction between the basal cells and the spinous keratinocytes also becomes less precise in the JCB-110 as the dose level increases. Thus, the toxicity of naphthalene is reflected by the morphological changes in the skin structure.

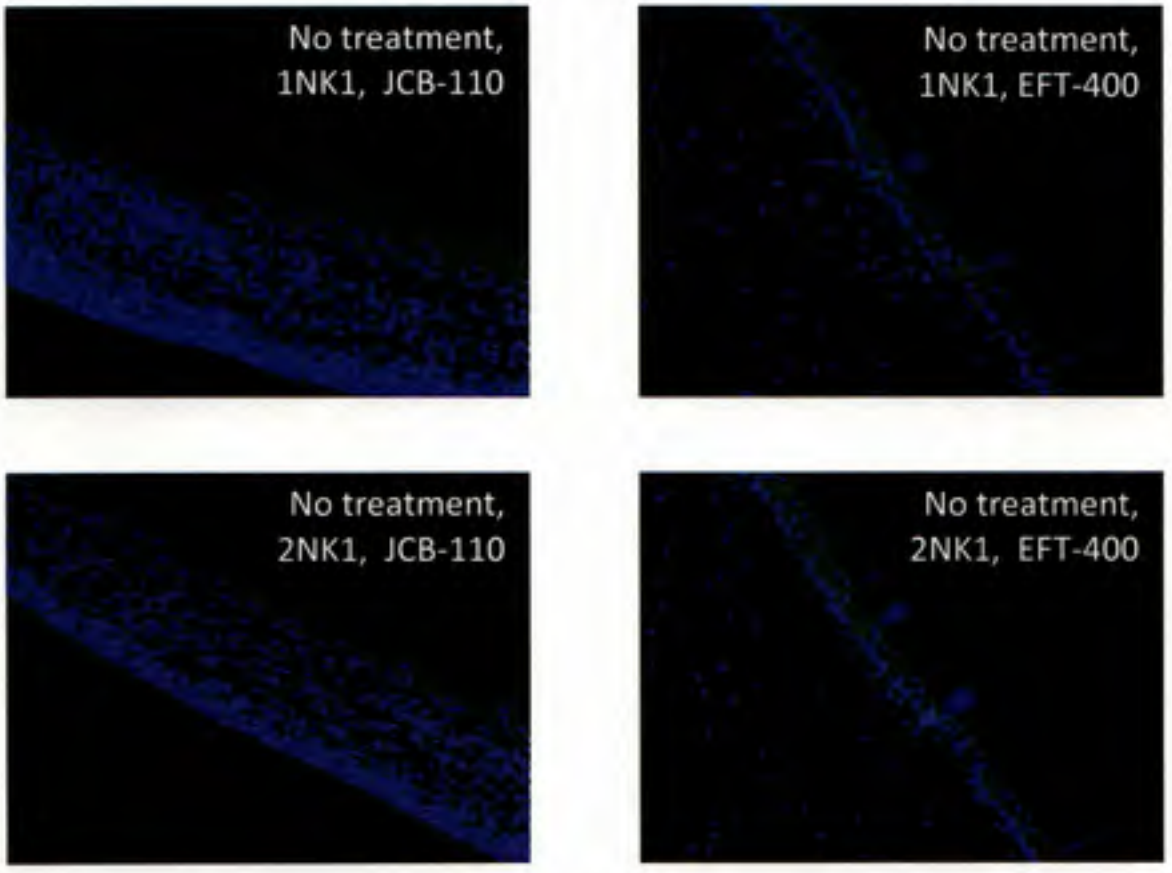

Figure 8. Unexposed JCB-110 (left) and EFT-400 (right) reconstructs do not show any 1NK1 and 2NK1-adducts. JCB-110 reconstructs contain more compact fibroblasts compared to the dispersion of fibroblasts seen in the dermis of the EFT-400 reconstructs. The epidermis and dermis are more defined in the EFT-400 reconstructs.

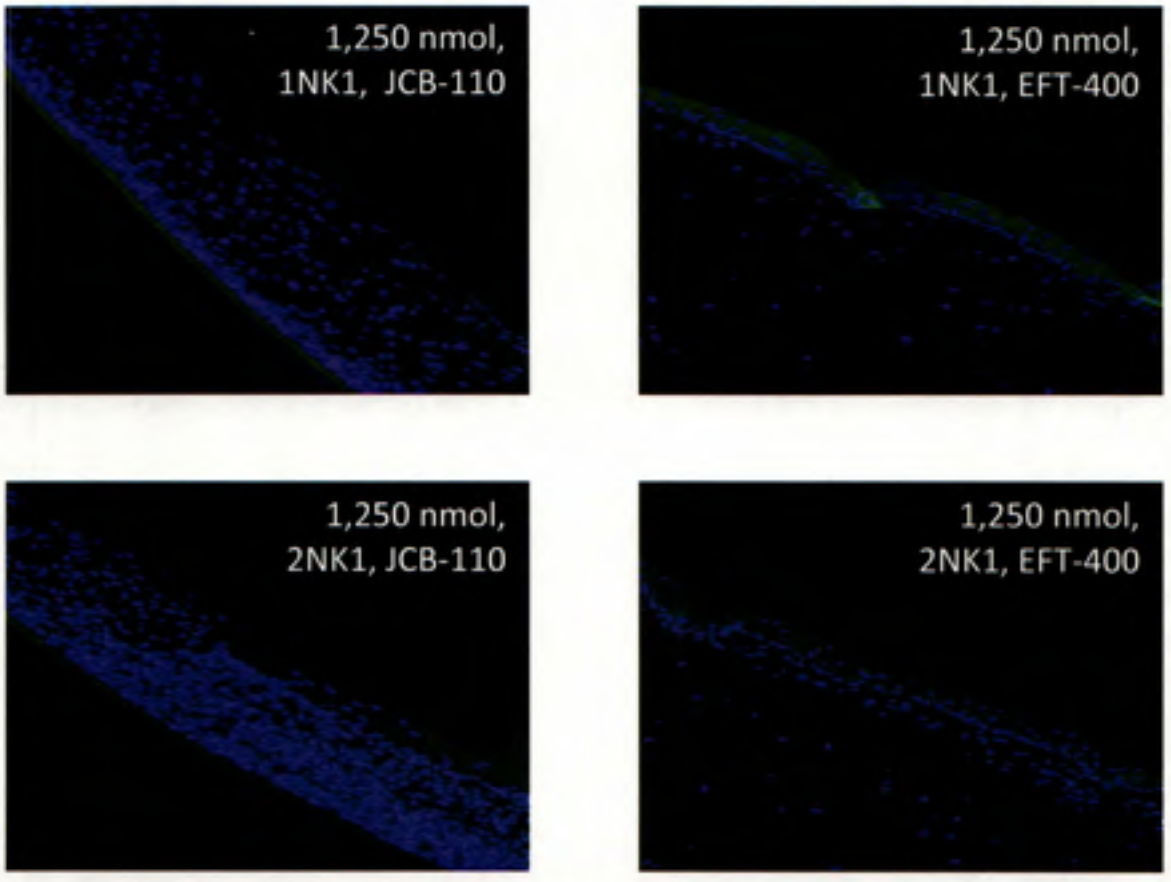

Figure 9. JCB-110 (left) and EFT-400 (right) reconstructs exposed to 1,250 nmol of naphthalene showed some 1NK1- and 2NK1-adducts (green). At this dose level, the 1NK1- and 2NK1-adducts are present in the basal layer of the epidermis were viable keratinocytes are present, but not in the stratum corneum.

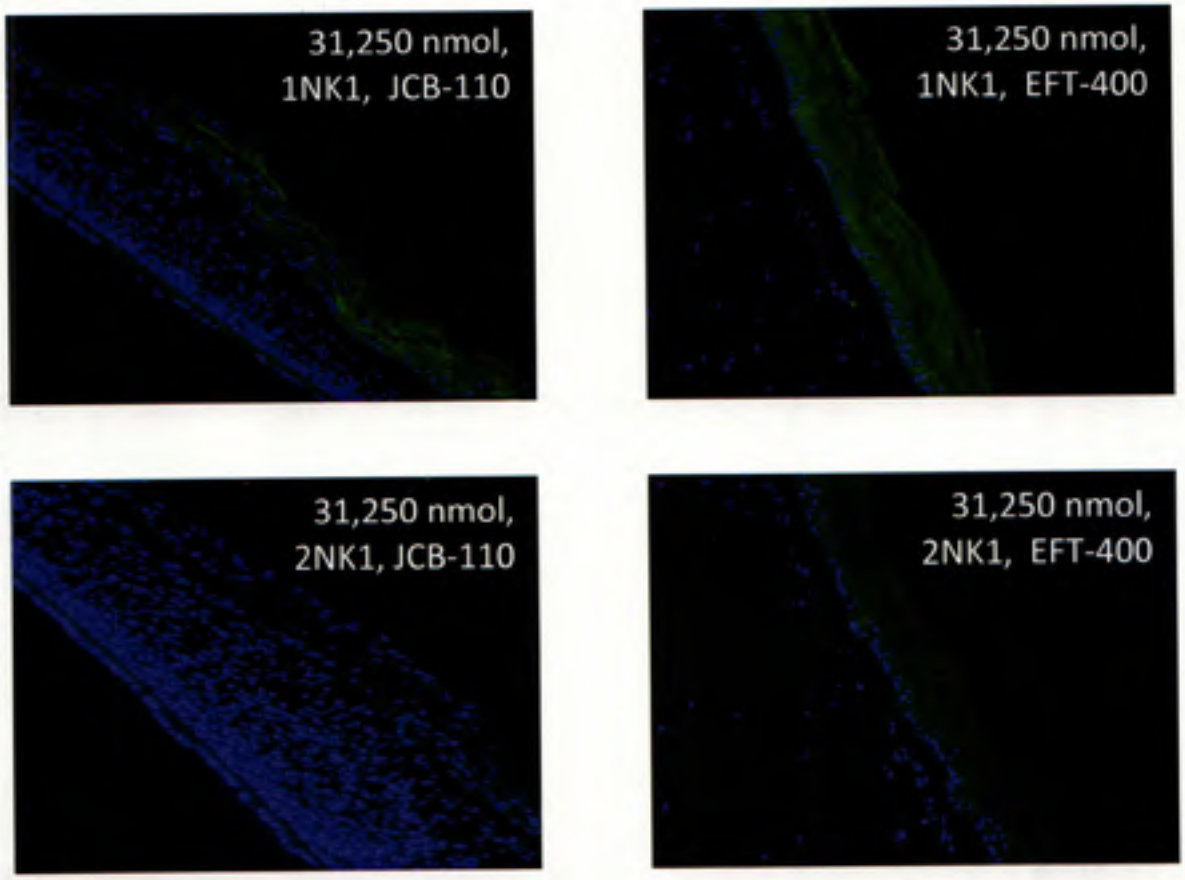

Figure 10. JCB-110 (left) and EFT-400 (right) reconstructs exposed to 31,250 nmol of naphthalene showed 1NK1- and 2NK1-adducts (green) throughout the epidermis including the stratum corneum. The distinction between the basal cells and the spinous keratinocytes becomes imprecise in the JCB-110 reconstructs.

CHAPTER IV

DISCUSSION

A review of the peer-reviewed scientific literature revealed that current methods for investigating the effects of dermal exposure are often not representative of human exposure scenarios. In addition, the results presented in these different studies are difficult to compare due to vastly different methodologies and models employed by the investigators (Scheiber et al., 2005). My goal in this study was to demonstrate the potential for 3D human *in vitro* skin reconstructs as a suitable model and surrogate to investigate the effects of xenobiotic exposure on human skin. The advantages of using skin reconstructs as a model for human skin is that the physical variables of tissue can be controlled and the obtained results may be more comparable between studies.

To achieve this goal, I began with showing that the EFT-400 reconstructs performed as a barrier by impeding the efflux of naphthalene and metabolites into the media. Using the EFT-400 reconstructs, I was then able to show that naphthalene was being metabolized and that 1-NAP and 2-NAP were being sequestered in the epidermis by adduction to keratin and less than one percent of naphthalene or naphthalene metabolite equivalents were found in the media. I then showed that the JCB-110 reconstructs prepared in our laboratory performed in the similar manner as the EFT-400 reconstructs.

4.1 Naphthalene Disposition

This series of experiments using naphthalene to characterize 3D human *in vitro* skin reconstructs provide some interesting results. The limited amount of naphthalene and 1,2-DHN that were

observed in the media and the polycarbonate membrane as well as the presence of naphthyl-keratin adducts in the epidermis suggests that the epidermis serves as a barrier to naphthalene. The amount of naphthalene that was present in the polycarbonate membrane (0.14 %), relative to the 0.08% of naphthalene found in the media also suggests that naphthalene may accumulate inside the plastic wells in which the skin reconstructs were dosed.

4.2 Immunohistochemistry Assay for Naphthyl-Keratin Adducts

The presence of naphthyl-keratin adducts in the epidermis demonstrate metabolism and a mechanism of elimination by desquamation. The significance of this experiment is that metabolism occurred in the reconstructs indicating normal cells/tissue functions. It is also important to note that naphthols that are bound to keratin would not reach the media (or systemic circulation *in vivo*). An increase in fluorescence was observed in both the EFT-400 and JCB-110 reconstruct models with respect to the naphthalene dose applied. This dose response suggests that cell viability and enzyme expression are not being negatively impacted at the exposure levels of 1,250, 6,250, and 12,500 nmol. Structural effects were observed in the JCB-110 reconstructs treated with 31,250 nmol of naphthalene. The uniformity of the JCB-110 stratum corneum became less distinct. This change was also reflected in the amount of naphthyl-keratin adducts observed in the viable epidermis suggesting that the viability of keratinocytes in the basal layer was decreased and/or the pattern of metabolism of naphthalene to naphthols was changed.

4.3 Comparison of the Skin Reconstructs

A comparison of the two different types of skin reconstructs, EFT-400 and JCB-110, yielded nearly identical results in both rate and quantity with respect to the amount of naphthalene that absorbed into tissue and was subsequently found in the media. This is an indication that the properties of the tissue constructs are very similar in the commercially available and our in-house made tissues. The observed dose response demonstrates the ability of the epidermis in the reconstructs to sequester large amounts of naphthalene. There was no dose related damage observed until the 31,250 nmol dose regimen. The damage to the epidermis after exposure to the 31,250 nmol dose regimen was observed only in the JCB-110 reconstructs.

4.4 Study Limitations

I recognize that the experiments conducted in this study had some limitations. A quantitative account of naphthalene distribution was not performed. In this study, we demonstrated that only a small amount of naphthalene effluxes the reconstruct into the media and that naphthyl-keratin adducts are present in the epidermis, however we do not know the amount of naphthalene that is metabolized and sequestered in this manner. We have not accounted for the possible adduction to proteins other than keratin, the potential for interaction between naphthalene and collagen in the dermis, or losses due to evaporation and/or reactions with plastic surfaces.

Enzyme activity and gene expression have not yet been demonstrated in the JCB-110 model and have only recently been characterized in the literature for commercially available models (Hu et al., 2010; Jackh et al., 2011). (Hu, et al., 2010) (Jackh, et al., 2011) Assays to determine gene expression and enzyme activities will be incorporated into future studies using 3D skin reconstructs.

4.5 Future Studies

A mass balance study should be performed when evaluating specific xenobiotics, such as naphthalene, with 3D skin reconstructs to determine how much and where loss can be attributed. It is possible that both loss to the plastic surfaces during dosing and evaporation during sample processing may have contributed to the observed results. Experiments conducted to determine the loss during the concentration process in ethyl acetate by nitrogen demonstrated that >50% of the spiked naphthalene amount evaporated. The use of a radiolabeled chemical could provide insight into where and how much chemical is retained in the epidermis and dermis of the reconstruct. This information would allow the determination of the most important areas to focus our efforts. If it is determined that there is little to no chemical in the epidermis and/or dermis, then there would not be any need to develop extraction methods for the tissues, for example.

Recent publications by Hu et al. (2010) and Jackh et al. (2011) have characterized gene expression in EpiDerm 3D models and human skin. Hu et al. (2010) observed that 84% of the enzymes found in a sample human skin were present in EpiDerm reconstructs. They also report that among the genes not observed in the EpiDerm model were the phase I enzymes CYP1A1, CYP2E1, and CYP2A6. This is of interest because these are among the enzymes postulated to be responsible for naphthalene metabolism. Jackh at al. (2011) confirmed that cytochrome P450 enzyme activity of CYP1A1, CYP2B6, and CYP3A4 were not detected in their follow up study. However, Jackh at al. (2011) did find that flavin-dependent monooxygenases 1 and 3 (FMO1 and FMO3) were active. The verification of gene expression and enzyme activities will need to be demonstrated when using 3D reconstructs for any given substrate. As for naphthalene, the

enzyme activities that are believed to be responsible for the metabolism of naphthalene in the JCB-110 model as well as in the EFT-400 model will be investigated in a future study. A study should also be conducted to determine if FMO1 and 3 oxidize naphthalene to produce the naphthyl-keratin adducts in the skin. In addition, the characterization of tissue reconstructs is needed to further optimize these test systems to be capable of demonstrating biotransformation xenobiotics (Neis et al., 2010).

Human 3D *in vitro* skin reconstructs have a great potential to provide a means to investigate gene-environment interactions in an *in vitro* environment via manipulation of genes and gene expression to model human disease. These manipulations could be beneficial when conducting research into populations that have increased susceptibility potential, such as individuals with mutations within the filaggrin gene (*FLG*). Filaggrin is a structural protein that contributes to the aggregation of the keratin cytoskeleton. Individuals with mutations to the *FLG* gene, which encodes for filaggrin expression have been associated with atopic dermatitis (AD). The lack of structure in the stratum corneum leads to gaps in the epidermis and possibly to an increased risk of higher absorption of dermal dose from a given exposure (Kawasaki et al., 2011). One possible experiment to test this theory would be to expose 3D skin reconstructs derived from cells from individuals with and without this mutation to naphthalene. The hypothesis would be that more naphthalene and naphthalene metabolites would efflux through the skin samples and into the media of the reconstructs prepared from individuals without the FLG mutation.

To consider the use of 3D reconstructs as a means of screening xenobiotics, a series of experiments and comparisons must be made in different matrices and with a variety of chemicals among the models currently used for measuring the toxic effects associated with xenobiotic

absorption. These models may include the use of mouse models and excised human skin to compare with results from 3D reconstructed skin with respect to metabolism observed, gene expression, and enzyme activity. Subsequent studies using separate dermal models will need to be performed to completely understand the mechanisms of exposure of any given xenobiotic.

4.6 Impact

This study is the first in a series to demonstrate that 3D human *in vitro* tissue reconstructs can be used to investigate the effects of xenobiotic exposures in humans. This study also provides an initial evaluation of the performance of JCB-110 reconstructs compared to the commercially available EFT-400 reconstructs with respect to naphthalene exposure. The structure and functionality of JCB-110 reconstructs performed as expected with regard to response to naphthalene exposure. The results from this study suggest that the metabolism of naphthalene in the skin results in formation of naphthyl-keratin adducts in the skin. Therefore, it is possible that the majority of metabolites observed in the urine and blood samples collected from naphthalene exposed individuals are mainly due to inhalation exposure and to minor extent from dermal exposure and/or naphthalene reaching systemic circulation due to saturation of the metabolic pathways in the skin.

CHAPTER V

CONCLUSION

This initial evaluation of 3D human *in vitro* skin reconstructs demonstrates their potential use as a model to screen for xenobiotic toxicity. The reconstructs metabolized and sequestered naphthalene in the suprabasal layer throughout the 5-day dosing regimen, therefore exhibiting minimal change in cell viability and tissue morphology during the multi-day exposure studies. The metabolism of naphthalene to naphthalene-1,2-oxide and subsequent adduction to keratin in the epidermis was demonstrated by the adduction of naphthalene to the keratin proteins and the absence of metabolites in the tissue culture media after exposure to naphthalene. Both the commercially available EFT-400 and the in-house grown JCB-110 reconstructs performed in a similar manner. These experiments will serve as a foundation for further development of the JCB-110 reconstructs and to optimize this model for toxicology and human exposure assessment studies.

References

Andreoli, C., Gigante, D., & Nunziata, A. (2003). A review of in vitro methods to asses the biological activity of tobacco smoke with the aim of reducing the toxicity of smike. *Toxicology in Vitro 17*, 587-594.

Balharry, D., Sexton, K., & BeruBe, K. A. (2008). An in vitro approach to assess the toxicity of inhaled. *Toxicology 244*, 66-78.

Brohem, C. A., da Silva Cardeal, L. B., Tiago, M., Soengas, M. S., de Moraes Barros, S. B., & Maria-Engler, S. S. (2010). Artificial skin in perspective: concepts and applications. *Piment Cell Melanoma Research 24*, 35-50.

Chao, Y. C., Kupper, L. L., Serdar, B., Egeghy, P. P., Rappaport, S. M., & Nylander-French, L. A. (2006). Dermal exposure to jet fuel JP-8 significantly contributes to the production of urinary naphthols in fuel-cell maintenance workers. *Environmental Health Perspectives 114*, 182-185.

Chao, Y.-C., Gibson, R. L., & Nylander-French, L. A. (2005). Dermal exposure to jet fuel (JP-8) in US Air Force personnel. *The Annals of Occupational Hygiene 49*, 639-645.

Chilcott, R. T. (2008). Cutaneous Anantomy and Function. In R. T. Chilcott, & S. Price , *Principles and Practice of Skin Toxicology* (pp. 3-16). Chichester, UK: John Wiley & Sons, Ltd.

Del Rio, M., Larcher, F., Serrano, F., Meana, A., Munoz, M., Garcia, M., et al. (2002). A preclinical model for the analysis of genetically modified human skin in vivo. *Humane gene therapy 13*, 959-968.

Eckert, R. L. (1991). The Structure and Function of Skin. In H. Mukhtar, *Pharmacology of the Skin* (pp. 4-10). Boca Raton: CRC Press.

Egeghy, P. P., Hauf-Cabalo, L., Gibson, R., & Rappaport, S. M. (2003). Benzene and naphthalene in air and breath indicators of exposure to jet fuel. *Occupational and Environmental Medicine 60*, 969-976.

Forbes, B., & Ehrhardt, C. (2005). Human respiratory epithelial cell culture for drug delivery applications. *European Journal of Pharmaceutics and Biopharmaceutics 60* (2), 193-205.

Foster, K. A., Avery, M. L., Yazdanian, M., & Audus, K. L. (2000). Characterization of the Calu-3 cell line as a tool to screen pulmonary drug delivery. *International Journal of Pharmaceutics 208*, 1-11.

Gibbs, S., van de Sandt, J. J., Merk, H. F., Lockely, D. J., Pendlington, R. U., & Pease, C. K. (2007). Xenobiotic metabolism in human skin and 3D human skin reconstructs: a review. *Current Drug Metabolism 8*, 758-772.

Hu, T., Khambatta, Z. S., Hayden, P. J., Bolmarcich, J., Binder, R. L., Robinson, M. K., et al. (2010). Xenobiotic metabolism gene expression in the Epiderm in vivo 3D human epidermis model compared to human. *Toxicology in vitro 24*, 1450-1463.

Jackh, C., Blatz, V., Fabion, E., Guth, K., van Ravenzwaay, B., Reisinger, K., et al. (2011). Characterization of enzyme activities of Cytochrome P450 enzymes, Flavin-dependent monooxygenases, N-acetyltransferases and UDP-glucuronyltransferases in human reconstructed epidermis and full-thickness skin models. *Toxicolgy in Vitro 25*, 1209-1214.

Kang-Sickel, J. C., Butler, M. A., Frame, L., Serdar, B., Chao, Y. C., Egeghy, P., et al. (2011). The utility of naphthyl-keratin adducts as biomarkers for jet-fuel exposure. *Biomarkers 16*, 590-599.

Kang-Sickel, J. C., Fox, D. D., Nam, T. G., Jayaraj, K., Ball, L. M., French, J. E., et al. (2008). S-arylcysteine-keratin adducts as biomarkers of human dermal exposure to aromatic hydrocarbons. *Chemical research in toxicology* 852-858.

Kang-Sickel, J. C., Stober, V. P., French, J. E., & Nylander-French, L. A. (2010). Exposure to naphthalene induces naphthyl-keratin adducts in human epidermis in vitro and vivo. *Biomarkers* 488-97.

Kawasaki, H., Kubo, A., Sasaki, T., & Amagai, M. (2011). Loss-of-Function Mutations within the Filaggrin Gene and Atopic Dermatitis. *Current Problems in Dermatology 41*, 35-46.

Kim, D., Andersen, M. E., & Nylander-French, L. A. (2006). Dermal absorption and penetration of jet fuel components in humans. *Toxicology Letters* 11-21.

Kim, D., Anderson, M. E., Chao, Y. C., Egeghy, P. P., Rappaport, S. M., & Nylander-French, L. A. (2007). . PBTK modeling demonstrates contribution of dermal and inhalation exposure components to end-exhaled breath concentrations of naphthalene. *Environmental Health Perspectives 115*, 894-901.

Neis, M. M., Wendel, A., Wiederholt, T., Marquardt , Y., Joussen , S., Baron , J. M., et al. (2010). Expression and induction of cytochrome p450 isoenzymes in human skin equivalents. *Skin Pharmacology and Physiology 23*, 29-39.

NRC. (2007). *Toxicity Testing in the 21st Century: A Vision and a Strategy.* Washington, D.C.: The National Academies Press.

Poet, T. S., & McDougal, J. N. (2002). Skin absorption and human risk assessment. *Chemico-Biological Interactions 140*, 19-34.

Rappaport, S., Waidyanatha, S., & Serdar, B. (2004). Napthalene and its Biomarkers as Measures of Occupational Exposure to Polycyclic Aromatic Hydrocarbons. *Journal of Environmental Monitoring 6*, 413-416.

Regnier, M., Patwardhan, A., Scheynius , A., & Schmidt , R. (1998). Reconstructed human epidermis composed of keratinocytes, melanocytes and Langerhans cells. *Medical & Biological Engineering and Computing 36*, 821-824.

Santiago-Walker, A., Li, L., Haass, N. K., & Herlyn, M. (2009). Melanocytes: From Morphology to Application. *Skin Pharmacology and Physiology 22*, 114-121.

Scheiber, S., Mahmoud, A., Vuia, A., Rubbelke, M. K., Schmidt, E., Schaller, M., et al. (2005). Reconstructed epidermis versus human and animal skin in skin absorption studies. *Toxicology in Vitro 19*, 813-822.

Scheuplien, R. J., & Blank, I. H. (1971). Permeability of the skin. *Physiological Review 51*, 702-747.

Schweizer, J. (1993). Murine Epidermal Keratins. In M. Darmon, & M. Blumenberg, *Molecular Biolgy of the Skin* (pp. 33-78). San Diego: Academic Press.

Serdar, B., Egeghy, P. P., Gibson, R., & Rappaport, S. M. (2004). Dose-dependent production of urinary naphthols among workers exposed to jet fuel (JP-8). *American Journal of Industrial Medicine 46*, 234-244.

Serdar, B., Egeghy, P. P., Waidyanatha, S., Gibson, R., & Rappaport, S. M. (2003). Urinary biomarkers of exposure to jet fuel (JP-8). *Environmental Health Perspestives 111*, 1760-1704.

Snyder, W. S., Cook, M. J., Nasset, N. E., Karhausen, L. R., Howells, G. P., & Tipton, I. H. (Eds.). (1992). *International Commission on Radiological Protection. Report of the Task Group on Reference* (Vol. 23). New York: Pergamon Press.

Sobus, J. R., McClean, M. D., Herrick, R. F., Waidyanatha, S., Nylander-French, L. A., Kupper, L. L., et al. (2009a). Investigation of PAH biomarkers in the urine of workers exposed to hot asphalt. *Annals of Occupational Hygiene 53*, 551-560.

Sobus, J. R., McClean, M. D., Herrick, R. F., Waidyanatha, S., Onyemauwa, F., Kupper, L. L., et al. (2009b). Comparing urinary biomarkers of airborne and dermal exposure to polycyclic aromatic compounds in asphalt-exposed workers. *Annals of Occupational Hygiene 53*, 561-571.

Tingle, M. D., Permohamed, M., Templeton, E., Wilson, A. S., Madden, S., Kitteringham, N. R., et al. (1993). An investigation of the formation of cytotoxic, genotoxic, protein-reactive and stable metabolites from naphthalene by human liver microsomes. *Biochemical Pharmacology 46*, 1529-1538.

Troester, M. A., Lindstrom, A. B., Waidyanatha, S., Kupper, L. L., & Rappaport, S. M. (2002). Stability of hemoglobin and albumin adducts of naphthalene oxide, 1,2-naphthoquinone, and 1,2-naphthoquinone. *Toxicological Sciences 68*, 314-321.

Waidyanatha, S., Zheng, Y., Serder, B., & Rappaport, S. M. (2004). Albumin Adducts of Naphthalene Metabolites as Biomarkers of Exposure to Polycyclic Aromatic Hydrocarbons. *Cancer Epidemiol Biomarkers & Prevention 1*, 117-124.

Wilson, A. S., Davis, C. D., Williams, D. P., Buckpitt, A. R., Pirmohamed, M., & Park, B. K. (1996). Characterisation of the toxic metabolite(s) of naphthalene. *Toxicology 114*, 233-242.

Zheng, J., Cho, M., Jones, A. D., & Hammock, B. D. (1997). Evidence of quinone metabolites of naphthalene covalently bound to sulfur nucleophiles of proteins of murine Clara cells after exposure to naphthalene. *Chemical Research in Toxicology 10*, 1008-1014.